

# VHF radar observations of nighttime *F*-region field-aligned irregularities over Kototabang, Indonesia

Y. Otsuka<sup>1</sup>, T. Ogawa<sup>1\*</sup>, and Effendy<sup>2</sup>

<sup>1</sup>*Solar-Terrestrial Environment Laboratory, Nagoya University, Japan*

<sup>2</sup>*National Institute for Aeronautics and Space, Bandung, Indonesia*

(Received December 6, 2007; Revised June 15, 2008; Accepted July 3, 2008; Online published May 14, 2009)

We report, for the first time, continuous observations of the nighttime *F*-region field-aligned irregularities (FAIs) over Indonesia. A VHF radar with operating frequency of 30.8 MHz and peak power of 20 kW has been operated at Kototabang (0.20°S, 100.32°E; dip latitude 10.4°S), Indonesia since February 2006. Five beams were allocated between  $\pm 54^\circ$  in azimuth around geographic south (126°–234°). From the continuous observation from February 2006 to November 2007, we found that FAIs appeared frequently at pre-midnight between March and May and at post-midnight between May and August. The pre-midnight FAIs coincided well with GPS scintillation observed at the same site. Seasonal and local time variations of the pre-midnight FAI occurrence are consistent with those of equatorial plasma bubbles reported in previous studies (e.g., Maruyama and Matuura, 1984). These results indicate that the pre-midnight FAIs could be associated with the equatorial plasma bubbles. On the other hand, seasonal and local time variations of the post-midnight FAIs were inconsistent with those of the plasma bubbles. The features of the post-midnight FAIs can be summarized as follows: (1) The post-midnight FAIs are not accompanied by GPS scintillations. (2) Most of the post-midnight FAI regions do not show propagation, but some of them propagate westward. (3) Echo intensity of the post-midnight FAIs was weaker than that of the pre-midnight FAIs. These features are similar to those of the FAI echoes that have been observed at mid-latitude (e.g., Fukao *et al.*, 1991). At Kototabang, Fukao *et al.* (2004) have firstly observed FAIs that resemble those at mid-latitude. The present paper reports statistical characteristics of the mid-latitude-type FAIs observed at Kototabang.

**Key words:** Equatorial ionosphere, field-aligned irregularity, VHF radar, GPS, scintillation.

## 1. Introduction

VHF-, UHF- and L-band radars near the geomagnetic equator have been used for observations of intense coherent echoes caused by Bragg scatter from field-aligned irregularities (FAIs) with a spatial scale-size of one half of the radar wavelength (e.g., Woodman and LaHoz, 1976; Tsunoda, 1980a, 1983). Spatial patterns of backscatter from FAIs are similar to those of equatorial plasma bubbles, and FAIs are collocated with plasma bubbles which are depletions in the equatorial *F* region plasma (e.g., Tsunoda, 1980b; Tsunoda *et al.*, 1982). The plasma bubbles are considered to be generated by the Rayleigh-Taylor instability at the bottom-side of the *F* region. Several coordinated observations of plasma bubbles and FAIs have been conducted (e.g., Rino *et al.*, 1981; Tsunoda *et al.*, 1982). Tsunoda (1980c) has compared spatial maps of plasma bubbles and FAIs by scanning the antenna beam in both incoherent and coherent measurements with the ALTAIR radar in the Kwajalein in the Central Pacific. They have shown that FAIs are collocated with plasma-depleted regions.

Within the plasma density depletions caused by the plasma bubbles, plasma density irregularities with various spatial scale-sizes exist (e.g., Basu *et al.*, 1978). A radio signal passing through small-scale irregularities in the ionospheric plasma density fluctuates in amplitude since the irregularities produce diffractive scattering. This phenomenon is known as amplitude scintillation. Scale-size of the irregularities which cause amplitude scintillations corresponds to the first-Fresnel scale shown by  $\sqrt{2\lambda z}$ , where  $\lambda$  is the radio wavelength and  $z$  is the altitude of the ionosphere. In the case of GPS radio wave, the Fresnel scale is approximately 300–400 m because the GPS L1 frequency is 1.57542 GHz and the ionospheric altitude is about 300–400 km. Therefore, plasma bubble occurrence can be detected by the GPS scintillation measurements (Ogawa *et al.*, 2009).

Recently, using Equatorial Atmosphere Radar (EAR) with operating frequency of 47 MHz at Kototabang (0.20°S, 100.32°E; dip latitude 10.4°S), Indonesia, which is located at magnetically low latitudes, FAIs in the nighttime *F* region has been studied (Fukao *et al.*, 2003a, b). Otsuka *et al.* (2004a) have conducted simultaneous two-dimensional observations of FAIs with 630-nm airglow depletions associated with equatorial plasma bubbles using an all-sky airglow imager, and shown that FAIs occur within the entire airglow-depleted region. Yokoyama *et al.* (2004) have in-

\*Now at National Institute of Information and Communications Technology, Tokyo, Japan.

vestigated relationship between onset of the *F* region FAIs and the sunset terminator. These FAIs are accompanied with the plasma bubbles. On the other hand, Fukao *et al.* (2004) have shown that some of FAIs resemble that observed with the MU radar at Shigaraki (34.9°N, 136.1°E; magnetic latitude: 25.6°), Japan at mid-latitudes.

In the mid-latitude nighttime *F* region, FAIs were detected by the MU radar (Fukao *et al.*, 1991) and by two VHF radars in the Caribbean sector (Swartz *et al.*, 2000). Mid-latitude FAIs are accompanied by medium-scale traveling ionospheric disturbances (MSTIDs), which have wavelengths of several hundred kilometers (Fukao *et al.*, 1991). Both MSTIDs and FAIs over Japan frequently occur during nighttime in summer (Saito *et al.*, 2002). They have wave-like structures with wavefront stretched from NW to SE and propagate southwestward.

As described above, the EAR is a powerful tool to observe FAIs over Indonesia. However, EAR is usually operated in a mode of troposphere and stratosphere measurements, and the ionospheric FAI measurements are made only approximately 4 weeks a year during seasons when plasma bubbles are expected to appear frequently. To make continuous observations of FAIs over Indonesia, we have installed a portable VHF radar at the EAR site. The present paper reports seasonal and local time variations of FAIs observed at Kototabang, Indonesia, which is located at magnetically low-latitude. The observed FAIs can be classified into two types; one is FAIs accompanied by equatorial plasma bubbles, and the other is FAIs similar to those observed at mid-latitudes.

## 2. Observation

We have operated routinely a VHF backscatter radar with operating frequency of 30.8 MHz at the EAR site, Kototabang since February 2006. The basic parameters are listed in Table 1. Peak and average transmitting power are 20 kW and 1.5 kW, respectively. The antenna is composed of a linear array of 18 three-element Yagi antennas with a total length of 117 m. The VHF radar has a capability to steer the radar beam to 9 directions between  $\pm 54^\circ$  in azimuth around geographic south ( $126^\circ$ – $234^\circ$ ). Zenith angle of all the radar beams is set at  $20^\circ$ . Half-power full beam width in azimuth and zenith directions are  $12^\circ$  and  $40^\circ$ , respectively. At Kototabang, as shown by Fukao *et al.* (2003a, b), the perpendicularity between the radar beam and geomagnetic field line can be achieved at beam zenith angle of  $24^\circ$  at due south and  $35^\circ$  at azimuth of  $\pm 54^\circ$  from due south. Within the half-power full beam width of  $40^\circ$  in zenith direction, the perpendicularity is achieved at all the 9 beam directions of the VHF radar.

The VHF radar was operated in a mode which consisted of *E* and *F* region FAI measurements. For the *F*-region FAI measurements, five beams with azimuth of  $125.8^\circ$ ,  $153.0^\circ$ ,  $180.0^\circ$ ,  $207.0^\circ$ , and  $234.2^\circ$  were steered to reveal spatial and temporal variations of the FAI echoes. This arrangement covered approximately 400 km in zonal direction at 400-km altitude. This coverage is almost same as the EAR multibeam measurements conducted by Fukao *et al.* (2004) and Otsuka *et al.* (2004a). The range and time resolutions of the VHF radar measurement were 19.2 km and about 4 min,

Table 1. Specifications of the VHF radar at Kototabang.

Location:	0.20°S, 100.32°E
Dip latitude	10.36°S
Operating frequency:	30.8 MHz
Antenna:	Linear array of 18 three-element Yagi antennas
Gain:	22 dBi
Beam width:	12° in azimuth (half-power full-width) 40° in zenith (half-power full-width)
Beam steering:	Active phase control Azimuthal beam directions between $+54^\circ$ and $-54^\circ$ at $13^\circ$ step
Transmitter:	Solid-state pulse transmitter
Peak power	20 kW
Average power:	1.5 kW
Pulse width:	1–200 $\mu$ s
Subpulse width:	1, 2, 4, 8, 16 $\mu$ s
Receiver:	Single coherent receiver
A/D converter	16 bit

Table 2. Observational mode for *F*-region FAI.

Parameter	Value
Azimuth of beams	$234.2^\circ$ , $207.0^\circ$ , $180.0^\circ$ , $153.0^\circ$ , $125.8^\circ$ from due north
Interpulse period	4 ms
Transmitted pulse	Single pulse with 128 $\mu$ s width
Number of coherent integration	4
Number of FFT points	128
Number of spectral average	3
Range resolution	19.2 km
Sampling interval	2.4 km
Range	122–544 km
Time resolution	4 min

respectively. Details of the observational mode is listed in Table 2.

## 3. Results

### 3.1 Seasonal and local time variations of FAI occurrence

By analyzing the *F*-region FAI data obtained with the VHF radar at Kototabang during a period from February 23, 2006 to November 28, 2007, we investigate seasonal and local time variations of the FAI echo occurrence rate. In this study, we use the radar backscatter echo with signal-to-noise ratio larger than 0 dB extending more than 50 km in range in order to exclude echoes other than FAIs. The signal-to-noise ratio was integrated from 200 to 540 km in range to investigate FAI occurrence rate. Figure 1(a) shows seasonal and local time variations of FAI echo intensity observed on the southward beam (azimuth of  $180^\circ$ ) during a period from February 2006 to November 2007. The black portion in the figure represents no observation due to instrumental problems. The figure indicates that FAIs appeared frequently at pre-midnight (between sunset and midnight) between March and May in 2006 and at post-midnight (between midnight and sunrise) between May and August in 2006 and 2007. The signal-to-noise ratio of the pre-midnight FAI echo tends to be larger than that of the

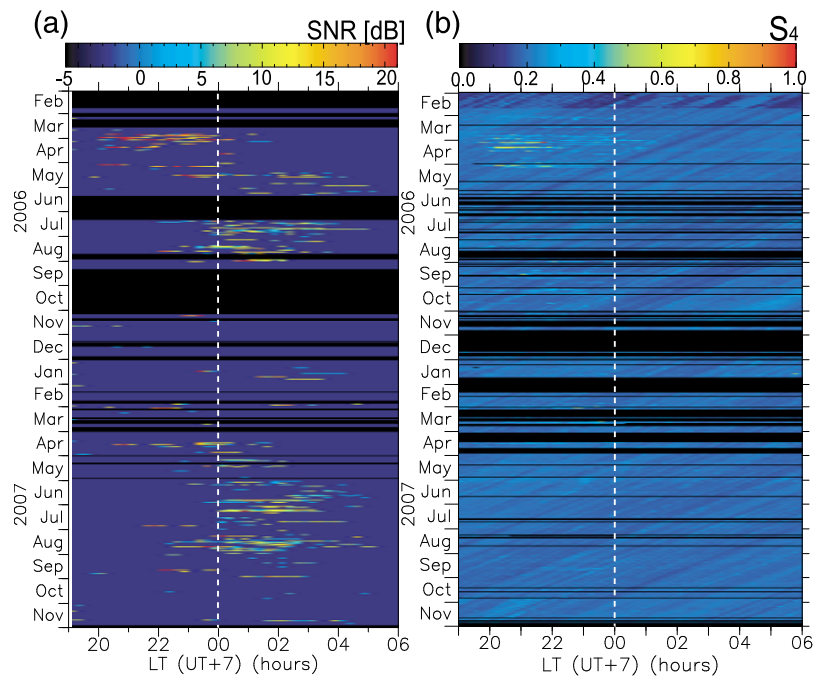


Fig. 1. Seasonal and local time variations of *F*-region FAI echo (a) and scintillation index ( $S_4$ ) (b) observed at Kototabang between February 2006 and November 2007.

post-midnight FAI echo.

### 3.2 Comparison with GPS scintillation occurrence

At the radar site, Kototabang, Indonesia, three single-frequency GPS receivers have been operated since January 2003 as part of a project titled “Coupling Processes in the Equatorial Atmosphere” to measure drift velocity of the ionospheric irregularities (Otsuka *et al.*, 2006; Ogawa *et al.*, 2009). The signal intensity of the GPS L1 frequency (1.57542 GHz) was sampled at a rate of 20 Hz to measure amplitude scintillation. GPS scintillation at the equatorial region could be caused by plasma density irregularities within equatorial plasma bubbles.

Scintillation index  $S_4$ , which is one of the parameters representing scintillation activity, was calculated every one minute using 1200 data points of the signal intensity data for one minute.  $S_4$  is defined as the standard deviation of the signal intensities divided by their mean. Figure 1(b) shows seasonal and local time variations of  $S_4$  during the same period shown in Fig. 1(a). To avoid multi-path effects of GPS signals, the data with elevation angles less than  $30^\circ$  were excluded, in the same way as Otsuka *et al.* (2006).  $S_4$  was averaged over 10 minute. The noise level of this  $S_4$  measurements is about 0.2. Scintillation occurrence rate was high between 2000–0100 LT around March equinox in 2006. This high occurrence rate coincided with the *F*-region FAI occurrence. However, GPS scintillation was not observed at post-midnight in May–August, when the *F*-region FAIs were observed by the VHF radar.

Otsuka *et al.* (2006) have analyzed GPS scintillation data obtained at Kototabang in two years (2003–2004) and revealed that the scintillations often occurred between 2000–0100 LT at equinoxes and that their occurrence rate was higher during March–April than during September–October. This equinoctial asymmetry in the GPS scintil-

lation occurrence rate is consistent with our observational results. However, the occurrence rate in 2006 and 2007 is lower than that in 2003–2004, and scintillation was observed only in a few days in 2007. This could be due to solar activity dependence of the plasma bubble occurrence because the solar activity decreases during a period from 2003 to 2007.

### 3.3 Examples of post-midnight FAIs

Figure 2 shows range-time-intensity (RTI) plots of the *F*-region FAI echoes observed on the five beams on the night of August 21, 2007. The vertical axis in the right-hand of each figure shows altitude at which the radar beam is perpendicular to the geomagnetic field. This figure shows an example of the post-midnight FAIs. FAI echoes on the beams with azimuth of  $180.0^\circ$ ,  $153.0^\circ$ , and  $125.8^\circ$  lasted for more than 4 hours during 2200–0400 LT while changing their altitude in the range from 200 to 350 km. Although temporal and altitude variations of the FAI echoes observed on the five beams are different, time delay of the FAI echoes between the different beams can not be seen. This result indicates that the FAIs did not move in the zonal direction.

Figure 3 shows RTI plots of the *F*-region FAI echoes observed on the night of July 8, 2007. On this night, FAI echoes were observed continuously during 2330–0300 LT on the easternmost beam and 0030–0500 LT on the westernmost beam. From this time delay, trace velocity of the echo region in the zonal direction is found to be 120 m/s westward.

Figure 4 shows RTI plots of the *F*-region FAI echo observed on the night of July 22, 2007. FAI echoes were observed during 0030–0300 LT and 0330–0430 LT. The former FAI echoes have a blob-like structure in the RTI plot. The echo region expanded to the altitude region from 200 to 400 km. Within the FAI echo region, striations with

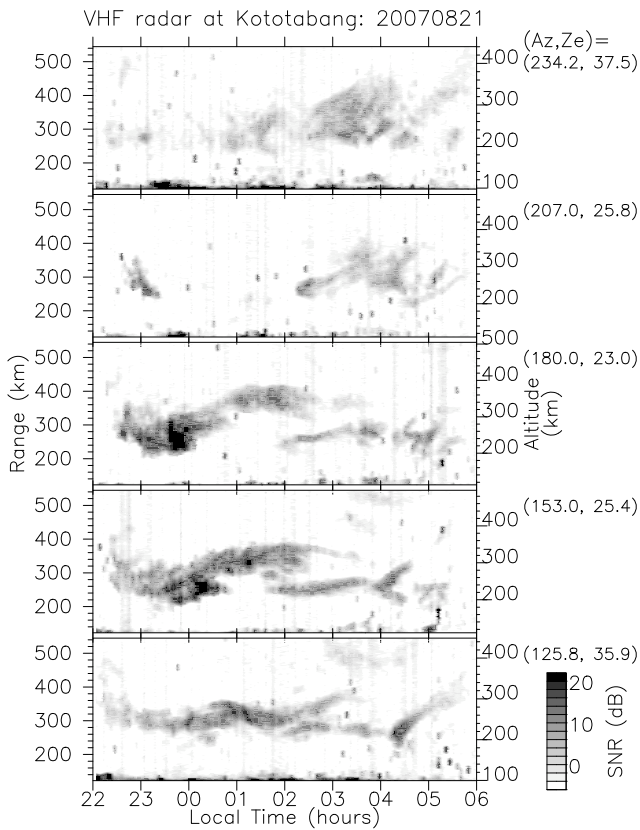


Fig. 2. Range-time-intensity plot of the Field-Aligned Irregularity (FAI) in the *F* region observed on the beam with azimuth of 234.2°, 207.0°, 180.0°, 153.0°, and 125.8° (from top to bottom panel) with the 30.8-MHz radar at Kototabang, Indonesia between 2200 LT on August 21, 2007 and 0600 LT on the subsequent day. Left vertical axis shows range from the radar and the right axis shows altitude at which the radar beam is perpendicular to the geomagnetic field.

positive slope can be seen. This indicates that the FAIs move upward. On the other hand, the latter FAI echo region was nearly horizontal elongated patches with altitude extension of approximately 30 km. This feature is similar to the FAIs observed by the MU radar, Japan (Fukao *et al.*, 1991). Fukao *et al.* (2004) reported that the Equatorial Atmosphere Radar (EAR) at Kototabang observed continuous FAI echoes which resemble those observed with the MU radar.

### 3.4 Propagation direction and Doppler velocity of FAI

East-west propagation direction of FAIs were investigated by comparing appearance of the FAI echoes between the different five beams. Some FAI echo regions changed their structures on the RTI plots during their passage through the field-of-view of the radar, corresponding to approximately 400 km in the zonal direction. In this case, it was difficult to determine time delay of the FAI echoes between the different beams. Especially, when plasma bubbles evolve rapidly after sunset, different stages of the plasma bubble development may be observed in the different beams. In this study, we used the data in which the time delay of FAI echoes was seen among more than three different beams. To compare the propagation directions between the pre-midnight and post-midnight FAIs, the data during a period from February 23, 2006 to Novem-

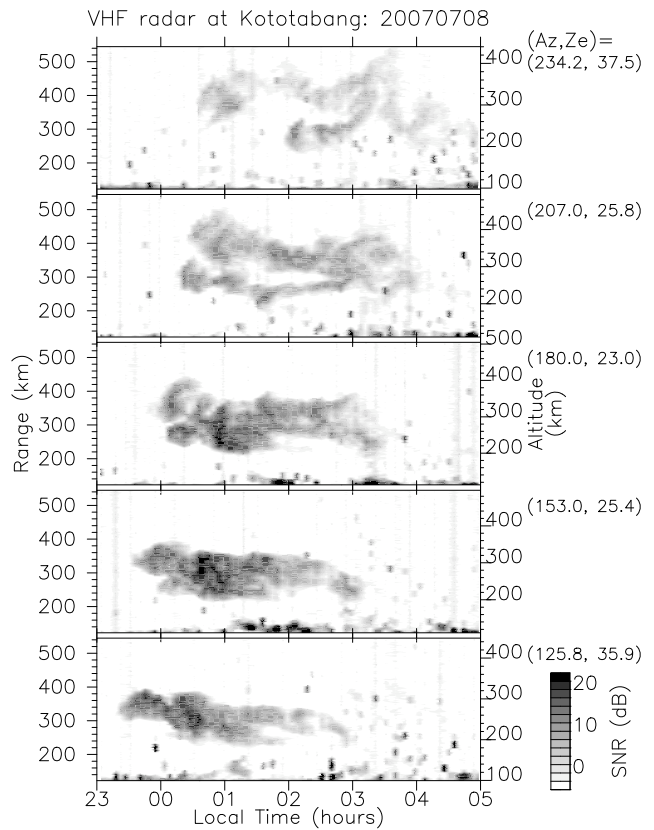


Fig. 3. Same as Fig. 2, but between 2300 LT on July 8, 2007 and 0500 LT on the subsequent day.

Table 3. Propagation direction of FAIs.

	FAI occurrence	Eastward	Westward	No propagation
Pre-midnight FAI	23 days	21 days (91%)	0 days (0%)	2 days (9%)
Post-midnight FAI	80 days	9 days (11%)	28 days (35%)	43 days (54%)

Pre-midnight FAI: 19–00 LT during March–May.

Post-midnight FAI: 00–06 LT during May–August.

ber 28, 2007 were classified into two groups; one is pre-midnight (19–00 LT) between March and May, and the other is post-midnight (00–06 LT) between May and August (Table 3). The pre-midnight and post-midnight FAIs were observed in 23 and 80 days, respectively. Number of days when pre-midnight (post-midnight) FAIs propagated eastward and westward are 21 and 0 (9 and 28), respectively. It is found that most of the pre-midnight FAIs propagated eastward. On the other hand, the post-midnight FAIs tended to propagate westward, although most of the post-midnight FAIs were stationary or did not show clear propagation (54%).

The Doppler velocity was obtained from the first-order moment of the FAI echo spectrum. All of the FAI observed at Kototabang during a period from February 2006 to November 2007 were classified into hourly bins, and the average Doppler velocity was obtained in each bin. Figure 5 shows local time variation of the averaged Doppler velocity observed on westernmost and easternmost (azimuth of 234°

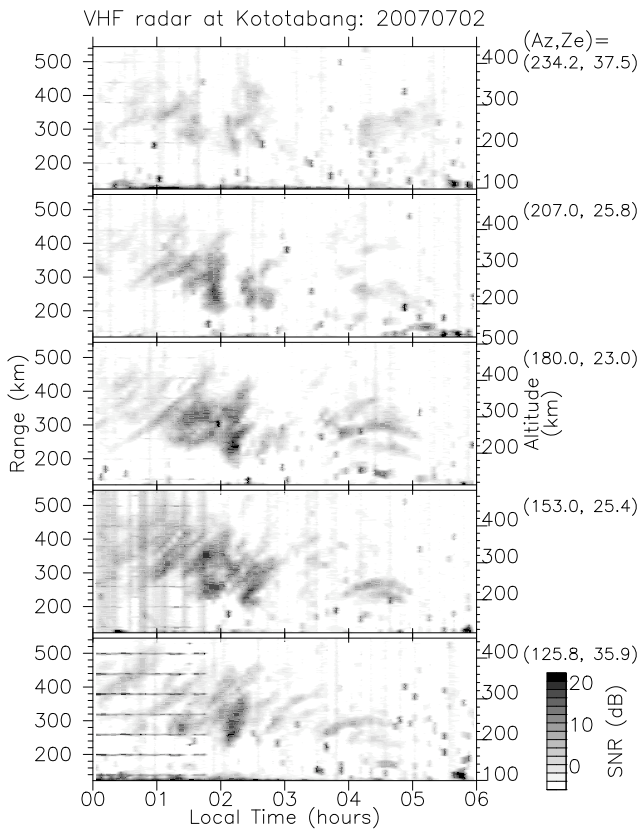


Fig. 4. Same as Fig. 2, but between 0000 LT 0600 LT on July 2, 2007.

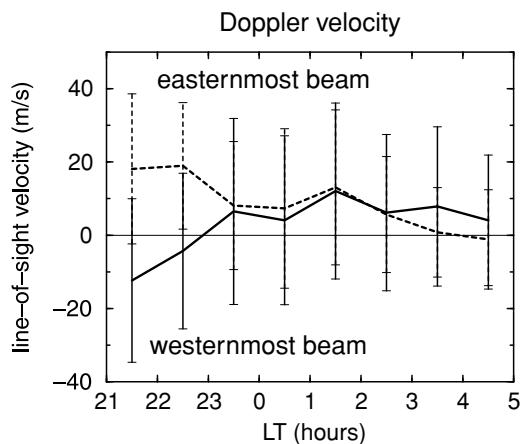


Fig. 5. Local time variations of average FAI Doppler velocity (positive away from the radar) observed on the westernmost beam (azimuth of 234.2°; solid curve) and easternmost beam (azimuth of 125.8°; dotted curve) of the 30.8-MHz radar at Kototabang. Error bar in the figure shows their standard deviation.

and 125°, respectively) beams. Positive (negative) value of the Doppler velocity indicates motion away from (toward) the radar. Error bars in the figure show their standard deviation. To reduce ambiguity of the velocity, the data with signal-to-noise ratio less than -5 dB are excluded. Since the Doppler velocity of the FAI echoes is the phase velocity of the plasma irregularities, the Doppler velocities are considered to correspond to line-of-sight component of the  $E \times B$  plasma drift. At pre-midnight, the Doppler velocity on the easternmost beam is positive and the Doppler veloc-

ity on the westernmost beam is negative. This result indicates that FAIs move eastward. Consequently, the propagation direction of the FAI region is same as that of  $E \times B$  plasma drift. On the other hand, at post-midnight, difference between the Doppler velocities on the westernmost and easternmost beams are less their standard deviations, and then distinct zonal drift velocities can not be seen.

#### 4. Discussion

Based on the characteristics of the FAIs observed with the VHF radar at Kototabang, the FAIs can be classified into the two groups, pre-midnight FAIs which are frequently observed at around equinox, and post-midnight FAIs which are frequently observed between May and August. Seasonal and local time variations of the pre-midnight FAI occurrence is consistent with those of the GPS scintillation occurrence, as shown in Fig. 1. Both the FAI radar echoes and scintillations could arise from plasma irregularities within the plasma bubbles. Seasonal variations of the plasma bubble occurrence rates, which depends on longitude, can be explained in terms of the geomagnetic field declination (Maruyama and Matuura, 1984; Tsunoda, 1985). Tsunoda (1985) described that plasma bubbles frequently occur under the condition that the sunset terminator is aligned with the declination. Maruyama and Matuura (1984) suggested that neutral winds which have a component parallel to the geomagnetic fields could suppress the plasma bubble occurrences. Because the magnetic field declination over Kototabang is close to zero, the plasma bubble occurrence rate is high at both March and September equinoxes. In actual, such seasonal variations were observed by the DMSP satellites (Burke *et al.*, 2004).

The FAI and GPS scintillation associated with the plasma bubbles were observed between 2000 and 0100 LT. Previous observations using all-sky airglow imagers show that 630-nm airglow intensity depletions caused by plasma bubbles exist during the whole night (e.g., Martinis *et al.*, 2003; Pimenta *et al.*, 2003). Scintillations of the VHF beacon radio waves were observed until sunrise (Valladares *et al.*, 1996). These results indicate that large-scale structures, which have more than a km scale-size, are maintained long after small scale irregularities disappear (Basu *et al.*, 1978). Basu *et al.* (1978) have shown that during generation phase of the equatorial irregularities in the evening hours, the kilometer and meter-scale irregularities coexist, whereas in the later phase, the meter-scale irregularities decay but the large-scale ones continue to exist.

On the other hand, post-midnight FAIs were frequently observed between May and August, when occurrence rate of the plasma bubble is low at the Indonesian longitudinal sector. Furthermore, FAIs within the plasma bubbles could disappear after midnight due to the plasma diffusion, as described above. Consequently, the post-midnight FAIs could not be associated with the plasma bubbles. Subbarao and Krishna Murthy (1994) and Chandra *et al.* (2003), who have investigated statistically spread-*F* occurrence rate over India, show that range-type spread-*F* occurs frequently at the post-sunset period in equinoxes especially during high solar activity whereas frequency-type spread-*F* is frequent at post-midnight in northern summer season during low solar

activity period. The range-type spread-*F* could be responsible for the plasma irregularities within the plasma bubbles. On the other hand, frequency-type spread-*F* occurs frequently at mid-latitudes. At the Japanese and Australian longitudinal sector, the frequency-type spread-*F* frequently occur in nighttime during May–August (Bowman, 1992). This seasonal variation of its occurrence rate is consistent with that of FAIs observed by the MU radar in Japan (Fukao *et al.*, 1991).

To observe the mid-latitude FAIs, powerful radars, such as the MU radar, are necessary because echo intensity from the mid-latitude FAIs is weaker than that from the FAIs within the plasma bubbles. Fukao *et al.* (1991) and Saito *et al.* (2002) have conducted multibeam measurements by the MU radar and shown that the FAI regions propagate westward. These features of the mid-latitude FAIs are similar to those of the post-midnight FAIs observed in Indonesia during May–August. Furthermore, as shown in Section 3.3, echo structures of the post-midnight FAIs in RTI plot resemble those of the mid-latitude FAIs. These results indicate that the mid-latitude FAIs can appear over Indonesia, which is located at magnetically low-latitude (dip latitude of 10.4°S).

At mid-latitudes, FAIs often coexist with MSTIDs. Both FAIs and MSTIDs have structures elongated from northwest to southeast and propagate southwestward (Saito *et al.*, 2002). The mid-latitude MSTIDs are associated with polarization electric fields (Shiokawa *et al.*, 2003; Otsuka *et al.*, 2004b). These polarization electric fields could play an important role in generating the FAIs through the gradient-drift instability. This may be a reason why the FAIs over Japan have structure similar to the MSTIDs and propagate to the same direction as the MSTIDs.

Shiokawa *et al.* (2002) have shown a case that equatorward limit of MSTIDs may exist around Okinawa (26.9°N; magnetic latitude: 18°), Japan. Kototabang is located at magnetically lower latitude than Okinawa, and corresponds to the location of the crest of the equatorial ionization anomaly. Therefore, such MSTIDs propagating southwestward may not appear at low-latitudes, such as Indonesia. Using an all-sky airglow imager at Kototabang, Shiokawa *et al.* (2006) observed MSTIDs whose occurrence rate is high during June–July, similar to the post-midnight FAIs. However, the propagation direction of the MSTIDs is magnetically poleward, and thus different from that of the post-midnight FAIs. Shiokawa *et al.* (2006) have suggested that the MSTIDs propagating poleward over Kototabang could be caused by gravity waves. Unlike the mid-latitude MSTIDs, these poleward-propagating MSTIDs could not be generated by polarization electric fields because of the following reason. Even if the polarization electric fields are generated by plasma density perturbations due to the MSTIDs to keep the current continuity, the electric fields are directed in the meridional direction since the poleward-propagating MSTIDs have wavefronts elongated in the zonal direction. The electric fields in the meridional direction move the plasma only horizontally, and then can not produce the plasma density perturbations (MSTIDs). Therefore, the poleward-propagating MSTIDs could not be caused by electric fields. This may be a reason why

MSTIDs over Kototabang is not associated with generation of post-midnight FAIs, unlike the mid-latitude MSTIDs.

Kotake *et al.* (2006) have shown seasonal and local time variations of the mid-latitude MSTIDs. The MSTIDs over Japan are active during a whole night of summer but they are most active at pre-midnight. Considering these results, we can speculate that the post-midnight FAIs over Kototabang may be FAIs which have been generated by the plasma density and electric field perturbations caused by MSTIDs at mid-latitudes and propagated to low-latitude.

Meter- and kilometer-scale irregularities in the ionosphere are considered to be generated by plasma instability, such as gradient-drift instability (e.g., Kelley, 1989). The instability could produce irregularities with continuous wavenumber spectrum. However, our observational result shows that the meter-scale FAIs observed over Kototabang at post-midnight were not accompanied by GPS scintillations caused by hundred-meter-scale irregularities. The mechanisms how the meter-scale FAIs observed over Kototabang at post-midnight are generated without larger scale irregularities are still unknown.

## 5. Summary and Conclusions

We have analyzed the data of *F*-region FAIs observed with a 30.8 MHz Doppler radar at Kototabang (0.20°S, 100.32°E; dip latitude 10.4°S), Indonesia during a period from February 23, 2006 to November 28, 2007. FAIs were observed frequently at pre-midnight between March and May and at post-midnight between May and August. The pre-midnight FAIs well coincided with GPS scintillation observed at the same site, and they could be accompanied by equatorial plasma bubbles. FAIs were also observed at post-midnight during May–August. The features of the post-midnight FAIs can be summarized as follows:

- 1) The post-midnight FAIs were not accompanied by GPS scintillation.
- 2) The post-midnight FAIs tended to propagate westward, although most of the post-midnight FAIs were stationary or did not show clear propagation (54%).
- 3) Echo intensity of the post-midnight FAIs is weaker than that of the pre-midnight FAIs.

These features are similar to those of the FAI echoes observed at mid-latitude.

**Acknowledgments.** This work is supported by Grant-in-Aid for Scientific Research (20684021) and on Priority Area (764) of the Ministry of Education, Culture, Sports, Science and Technology of Japan, and partly the 21st Century COE Program (Dynamics of the Sun-Earth-Life Interactive System, No. G-4) of Nagoya University, Japan. We thank Genesis Software for their kind support of the continuous radar operation.

## References

- Basu, S., Su, Basu, J. Aarons, J. P. McClure, and M. D. Cousins, On the coexistence of kilometer- and meter-scale irregularities in the nighttime equatorial *F* region, *J. Geophys. Res.*, **83**, 4219–4226, 1978.
- Bowman, G. G., Upper atmosphere neutral-particle density variations compared with spread-*F* occurrence rates at locations around the world, *Ann. Geophys.*, **10**, 676–682, 1992.
- Burke, W. J., L. C. Gentile, C. Y. Huang, C. E. Valladares, and S. Y. Su, Longitudinal variability of equatorial plasma bubbles observed by DMSP and ROCSAT-1, *J. Geophys. Res.*, **109**, A12301, doi:10.1029/

- 2004JA010583, 2004.
- Chandra, H., Som Sharma, M. A. Abdu, and I. S. Batista, Spread-*F* at anomaly crest regions in the Indian and American longitudes, *Adv. Space Res.*, **31**(3), 717–727, 2003.
- Fukao, S., M. C. Kelley, T. Shirakawa, T. Takami, M. Yamamoto, T. Tsuda, and S. Kato, Turbulent upwelling of the mid-latitude ionosphere, 1. Observational Results by the MU radar, *J. Geophys. Res.*, **96**, 3725–3746, 1991.
- Fukao, S., H. Hashiguchi, M. Yamamoto, T. Tsuda, T. Nakamura, M. K. Yamamoto, T. Sato, M. Hagino, and Y. Yabugaki, The Equatorial Atmosphere Radar (EAR): System description and first results, *Radio Sci.*, **38**(3), 1053, doi:10.1029/2002RS002767, 2003a.
- Fukao, S., Y. Ozawa, M. Yamamoto, and R. T. Tsunoda, Altitude-extended equatorial spread *F* observed near sunrise terminator over Indonesia, *Geophys. Res. Lett.*, **30**(22), 2137, doi:10.1029/2003GL018383, 2003b.
- Fukao, S., Y. Ozawa, T. Yokoyama, M. Yamamoto, and R. T. Tsunoda, First observations of the spatial structure of *F* region 3-m-scale field-aligned irregularities with the Equatorial Atmosphere Radar in Indonesia, *J. Geophys. Res.*, **109**, A02304, doi:10.1029/2003JA010096, 2004.
- Kelley, M. C., *The Earth's ionosphere, Plasma Physics and Electrodynamics*, Academic, San Diego, Calif., 1989.
- Kotake, N., Y. Otsuka, T. Tsugawa, T. Ogawa, and A. Saito, Climatological study of GPS total electron content variations caused by medium-scale traveling ionospheric disturbances, *J. Geophys. Res.*, **111**, A04306, doi:10.1029/2005JA011418, 2006.
- Martinis, C., J. V. Eccles, J. Baumgardner, J. Manzano, and M. Mendillo, Latitude dependence of zonal plasma drifts obtained from dual-site airglow observations, *J. Geophys. Res.*, **108**, 1129, doi:10.1029/2002JA009462, 2003.
- Maruyama, T. and N. Matuura, Longitudinal variability of annual changes in activity of equatorial spread *F* and plasma bubbles, *J. Geophys. Res.*, **89**, 10,903–10,912, 1984.
- Ogawa, T., Y. Miyoshi, Y. Otsuka, T. Nakamura, and K. Shiokawa, Equatorial GPS ionospheric scintillations over Kototabang, Indonesia and their relation to atmospheric waves from below, *Earth Planets Space*, **61**, this issue, 397–410, 2009.
- Otsuka, Y., K. Shiokawa, T. Ogawa, T. Yokoyama, M. Yamamoto, and S. Fukao, Spatial relationship of equatorial plasma bubbles and field-aligned irregularities observed with an all-sky airglow imager and the Equatorial Atmosphere Radar, *Geophys. Res. Lett.*, **31**, L20802, doi:10.1029/2004GL020869, 2004a.
- Otsuka, Y., K. Shiokawa, T. Ogawa, and P. Wilkinson, Geomagnetic conjugate observations of medium-scale traveling ionospheric disturbances at midlatitude using all-sky airglow imagers, *Geophys. Res. Lett.*, **31**, L15803, doi:10.1029/2004GL020262, 2004b.
- Otsuka, Y., K. Shiokawa, and T. Ogawa, Equatorial ionospheric scintillations and zonal irregularity drifts observed with closely-spaced GPS receivers in Indonesia, *J. Meteor. Soc. Jpn.*, **84A**, 343–351, 2006.
- Pimenta, A. A., P. R. Fagundes, Y. Sahai, J. A. Bittencourt, and J. R. Abalde, Equatorial *F*-region plasma depletion drifts: latitudinal and seasonal variations, *Ann. Geophys.*, **21**, 2315–2322, 2003.
- Rino, C. L., R. T. Tsunoda, J. Petriceks, R. C. Livingston, M. C. Kelley, and K. D. Baker, Simultaneous rocket-borne beacon and *in situ* measurements of equatorial spread-*F*—intermediate wavelength results, *J. Geophys. Res.*, **86**, 2411–2420, 1981.
- Saito, A., M. Nishimura, M. Yamamoto, S. Fukao, T. Tsugawa, Y. Otsuka, S. Miyazaki, and M. C. Kelley, Observations of traveling ionospheric disturbances and 3-m scale irregularities in the nighttime *F*-region ionosphere with the MU radar and a GPS network, *Earth Planets Space*, **54**, 31–44, 2002.
- Shiokawa, K., Y. Otsuka, M. K. Ejiri, Y. Sahai, T. Kadota, C. Ihara, T. Ogawa, K. Igarashi, S. Miyazaki, and A. Saito, Imaging observations of the equatorward limit of midlatitude traveling ionospheric disturbances, *Earth Planets Space*, **54**, 57–62, 2002.
- Shiokawa, K., Y. Otsuka, C. Ihara, T. Ogawa, and F. J. Rich, Ground and satellite observations of nighttime medium-scale traveling ionospheric disturbance at midlatitude, *J. Geophys. Res.*, **108**(A4), 1145, doi:10.1029/2002JA009639, 2003.
- Shiokawa, K., Y. Otsuka, and T. Ogawa, Quasi-periodic southward-moving waves in 630-nm airglow images in the equatorial thermosphere, *J. Geophys. Res.*, **111**, A06301, doi:10.1029/2005JA011406, 2006.
- Subbarao, K. S. V. and B. V. Krishna Murthy, Seasonal variations of equatorial spread-*F*, *Ann. Geophys.*, **12**, 33–39, 1994.
- Swartz, W. E., M. C. Kelley, J. J. Makela, S. C. Collins, E. Kudeki, S. Franke, J. Urbina, N. Aponte, M. P. Sulzer, and S. A. Gonzalez, Coherent and incoherent scatter radar observations during intense mid-latitude spread *F*, *Geophys. Res. Lett.*, **27**, 2829–2832, 2000.
- Tsunoda, R. T., Backscatter measurements of 11-cm equatorial spread-*F* irregularities, *Geophys. Res. Lett.*, **7**, 848–850, 1980a.
- Tsunoda, R. T., Magnetic-field-aligned characteristics of plasma bubbles in the nighttime equatorial ionosphere, *J. Atmos. Terr. Phys.*, **42**, 743–752, 1980b.
- Tsunoda, R. T., On the spatial relationship of 1-m equatorial spread *F* irregularities and plasma bubbles, *J. Geophys. Res.*, **85**, 185–190, 1980c.
- Tsunoda, R. T., On the generation and growth of equatorial backscatter plumes 2. Structuring of the west walls of upwellings, *J. Geophys. Res.*, **88**, 4869–4874, 1983.
- Tsunoda, R. T., Control of the seasonal and longitudinal occurrence of equatorial scintillations by the longitudinal gradient in integrated *E* region Pedersen conductivity, *J. Geophys. Res.*, **90**, 447–456, 1985.
- Tsunoda, R. T., R. C. Livingston, J. P. McClure, and W. B. Hanson, Equatorial plasma bubbles: Vertically elongated wedges from the bottomside *F* layer, *J. Geophys. Res.*, **87**, 9171–9180, 1982.
- Valladares, C. E., R. Sheehan, S. Basu, H. Kuenzler, and J. Espinoza, The multi-instrumented studies of equatorial thermosphere aeronomy scintillation system: Climatology of zonal drifts, *J. Geophys. Res.*, **27**, 26,839–26,850, 1996.
- Woodman, R. F. and C. LaHoz, Radar observations of *F*-region equatorial irregularities, *J. Geophys. Res.*, **81**, 5447–5466, 1976.
- Yokoyama, T., S. Fukao, and M. Yamamoto, Relationship of onset of equatorial *F*-region irregularities with sunset terminator observed with the Equatorial Atmosphere Radar, *Geophys. Res. Lett.*, **31**, L24804, doi:10.1029/2004GL021529, 2004.

---

Y. Otsuka (e-mail: otsuka@stelab.nagoya-u.ac.jp), T. Ogawa, and Ef-fendy